

# Fabrication of free-standing casein devices with micro- and nanostructured regular and bioimprinted surface features

Azadeh Hashemi, Isha Mutreja, Maan M. Alkaisi, and Volker Nock<sup>a)</sup>

*Department of Electrical and Computer Engineering, The MacDiarmid Institute for Advanced Materials and Nanotechnology, University of Canterbury, Christchurch 8140, New Zealand*

Mohammad Azam Ali

*Department of Applied Sciences, University of Otago, Dunedin 9054, New Zealand*

(Received 28 June 2015; accepted 8 September 2015; published 21 September 2015)

This work introduces a novel process for the fabrication of free-standing biodegradable casein devices with micro- and nanoscale regular and biomimetic surface features. Fabrication of intermediate polydimethylsiloxane (PDMS) moulds from photoresist masters and liquid-casting of casein is used to transfer arbitrary geometrical shapes onto the surface of casein devices. Casein film composition was optimized for mechanical stability and pattern resolution. It was found that 15% casein in 0.2% NaOH solution, mixed with 10% glycerol, and cross-linked by addition of 2% glutaraldehyde produced the best pattern transfer results. Biomimetic cell-like shapes were transferred onto casein by use of bioimprinting of two-dimensional cell-cultures into PDMS. To demonstrate this process, C2C12 mouse myoblasts were cultured on microscope slides, replicated into PDMS and casein using liquid casting and drying. Recessed alignment grids were integrated into the microscope glass slides to facilitate direct comparison of original cells and their bioimprints on PDMS and casein. Optical microscopy and atomic force microscopy confirmed the transfer of micron-scale morphological features, such as cell outlines, nuclei and larger lamellipodia, into the casein surface. Nanoscale feature resolution in casein was found to be limited compared to the PDMS intermediate moulds, which was attributed to limited wetting of the aqueous casein solution. Strategies to increase resolution of the casein transfer step, as well as degradation behavior of the fabricated devices in cell culture media are currently underway. Substrates fabricated with this process have applications in stem cell engineering, regenerative medicine, and implantable devices. © 2015 American Vacuum Society. [<http://dx.doi.org/10.1116/1.4931591>]

## I. INTRODUCTION

Surface topography is increasingly recognized as an important parameter, which can influence the development and function of biological cells. Mammalian cells cultured on engineered surfaces, with either, regular micro- and nanoscale patterns<sup>1-3</sup> or bioimprinted<sup>4-8</sup> cell-like features, have been shown to behave differently than cells cultured on flat surfaces. To this date, high-resolution surface patterning for biomedical applications has been confined to conventional tissue engineering plastics, such as polystyrene (PS), and specific metals used for medical implants.<sup>9</sup> Recently, plastics based on casein, the main protein of cow's skimmed milk, have been gaining renewed interest. First introduced in the early 20th century, casein-based polymers are both renewable and biodegradable.<sup>10</sup>

Micron-scale devices made of casein have since been proposed for use as degradable, stand-alone orthopedic implants<sup>11</sup> and tissue engineering substrates.<sup>12</sup> While a strong mechanical microstructure and no toxicity make casein a suitable material for implantation, acute inflammatory reactions of the surrounding tissue remain a problem.<sup>11</sup> To influence, and potentially ease reaction of the surrounding tissue,<sup>8</sup> we propose the incorporation of regular geometric and biomimetic tissuelike surface features into the cross-linked protein surface.

Existing techniques for the fabrication of casein-based devices have mainly focused on spin-coating of thin films<sup>13</sup> and casting of flat films from solution.<sup>14</sup> It has also been shown that three-dimensional freestanding structures with millimeter dimensions can be formed. In particular, repeated dip-coating of a rotating mandrel was used to form cylindrical tubes with millimeter diameter and controlled wall thickness.<sup>11</sup> These so called glutaraldehyde-cross-linked casein conduits (GCCs) were successfully implanted into adult rats and shown to promote regeneration after peripheral nerve injury coupled with controlled implant degradation over time.

To transfer integrated geometric patterns onto the surface of such devices, we have recently developed a replica-casting technique capable of reproducing lithographically defined micro- and nanoscale surface patterns on casein polymers.<sup>15</sup> In this paper, we introduce the replication process and demonstrate the fabrication of freestanding, biodegradable protein devices with micron- and nanometer-scale regular geometric surface patterns and positive and negative cellular bioimprints.

## II. EXPERIMENTAL SETUP AND METHOD

### A. Casein optimization

Casein (C7078-500G, Sigma-Aldrich) was purchased as powder. Depending on the buffer it was to be dissolved in, the influence of casein concentration and the type and concentration of plasticizer on resulting film characteristics

<sup>a)</sup>Electronic mail: volker.nock@canterbury.ac.nz

were investigated. In the present work, casein was dissolved in two different buffers, 3% disodium hydrogen phosphate buffer ( $\text{Na}_2\text{HPO}_4$ ) and 0.2% sodium hydroxide buffer (NaOH). The solutions were made of 10%, 15%, and 20% of casein and 0%, 10%, 20%, 30%, and 40% of glycerol as the plasticizer. To increase the stability, casein films were cross-linked. To determine the best method, three different cross-linking techniques were investigated. First, samples were made by immersing casein films in 0.1% glutaraldehyde solution, a cross-linking agent for proteins, for half an hour. Second, by adding 2% glutaraldehyde to the solution and third by immersing casein films in 3% citric acid solution for half an hour.

## B. Regular patterns

Regular micron- and nanoscale geometric patterns were transferred into casein from mould masters fabricated using photo- and interference lithography, respectively. A schematic of the process is shown in Fig. 1(a).

### 1. Mould master fabrication

*a. Photolithography.* Photolithography was used to transfer micron-scale 2.5D geometric shapes from a mask onto the surface of a silicon wafer. First, a laser mask writer ( $\mu\text{PG101}$ , Heidelberg Microsystems) was used to transfer regular test patterns, designed using software (L-Edit V16, Tanner), onto a chrome coated glass mask. A 4 in. silicon wafer was prepared by spin-coating a layer of AZ1518 photoresist at 2000 rpm for 60 s and then baking it at  $100^\circ\text{C}$  for 90 s on a hotplate. The mask was then placed in a mask aligner (Suss MA6 Mask Aligner), and the patterns were transferred onto the wafer via 15 s UV exposure. After development with AZ326 MIF developer for 45 s and rinsing with deionized water (DI), the resist was hard-baked at  $120^\circ\text{C}$  for 120 s.

*b. Interference lithography.* Interference lithography was used to prepare mould masters with nanoscale test patterns in photoresist. First,  $20 \times 20$  mm silicon substrates were prepared by spin-coating a layer of AZ1518 photoresist at 2000 rpm for 60 s and then baking it at  $100^\circ\text{C}$  for 90 s on a hotplate. A custom Lloyd's Mirror setup with 325 nm HeCd laser as light source was used to expose the resist.<sup>16</sup> Single exposure was used to produce 500 nm wide lines, and double exposure was used by  $90^\circ$  rotation to produce dot arrays. After development with AZ326 MIF developer for 45 s and rinsing with DI-water, the resist was hard-baked at  $120^\circ\text{C}$  for 120 s.

### 2. Casting of PDMS

Mould fabrication was followed by replica-casting with PDMS. First, PDMS prepolymer (Sylgard 184, Dow Corning) was mixed at a 10:1 w/w ratio, degassed, and poured onto the mould. It was then cured for 2 h at  $80^\circ\text{C}$  on a hotplate. After curing, the PDMS mould was peeled-off the

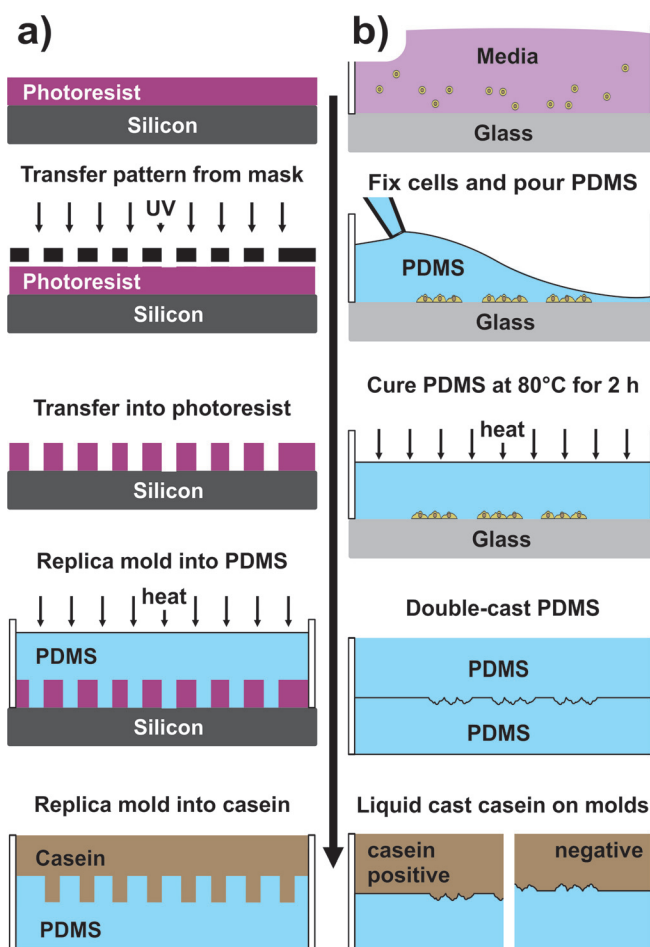


Fig. 1. (Color online) Schematic of the substrate patterning process using photolithography (a) and bioimprinting (b) to fabricate the initial pattern. For (a), photoresist is spin-coated on a silicon wafer. A prefabricated optical mask is then placed over the wafer and exposed using UV light. Alternatively, mask-less interference-lithography is used. The photoresist is developed to transfer patterns. PDMS is dispensed on the layer of photoresist and thermally cured. Patterns are transferred onto casein films by liquid-casting casein on the PDMS mould. In case of (b), cells are cultured on the microscope slides, fixed, and PDMS is dispensed onto the cells. PDMS is then thermally cured and peeled off. A second replica is made of the negative PDMS mould to form a positive mould. Positive and negative casein patterns are made by liquid-casting of the negative and positive PDMS moulds, respectively.

masters and further cross-linked by baking for an additional 2 h at  $80^\circ\text{C}$ .

### 3. Casein patterning

In order to transfer the regular patterns onto casein films, casein solution was liquid-cast on the PDMS moulds and left to dry overnight at room temperature. Prior to casein casting, PDMS moulds were plasma-treated for 30 s in 100 W oxygen plasma (K1050X Plasma Etcher, Quorum Emitech). Finally, cured casein was peeled-off the PDMS mould.

## C. Bioimprints

Cell-like patterns with micron- and nanometer-scale resolution were transferred into casein using bioimprinting. A schematic of the process is shown in Fig. 1(b).

### 1. Culture device fabrication

Microscope slides with grid patterns were used as cell culture substrates. In order to pattern the slides with a grid, a laser mask writer ( $\mu$ PG101, Heidelberg Microsystems) was used to transfer the grid design onto a chrome coated glass mask as described above. Microscope slides were spin-coated with AZ1518 photoresist at 2000 rpm and acceleration of 1000 rpm/s for 60 s. The mask was then placed over the microscope slides in the mask aligner and exposed to UV light for 15 s. Following this, the microscope slides were developed in AZ326 MIF developer and washed with DI-water. They were then baked for 10 min at 100 °C and grid patterns were etched into glass by immersing the slides into hydrofluoric acid for 2 min. The AZ1518 layer was finally stripped using acetone. Prior to use, the glass slides were sterilized using UV light.

### 2. Cell culture

Rat muscle cells (C2C12 myoblasts) were obtained from the University of Otago, Christchurch School of Medicine. Freshly isolated cells were designated with a passage number zero. Results presented in this work were obtained using cells with a passage number of 36. Working media were prepared by adding 10% fetal bovine serum (FBS, Life Technologies), 1% penicillin–streptomycin (P/S, Life Technologies), and 1% Fungizone to Dulbecco's modified Eagle's medium (DMEM, Life Technologies). Approximately 250 000 cells were placed on a 2.5 × 7.5 cm microscope slide with grid pattern and cultured in a cell-culture incubator for 24 h. The media was then removed, cells were washed with phosphate-buffered saline (PBS, Life Technologies), then fixed by adding paraformaldehyde fixative (Life Technologies), and left for 30 min. The fixative solution was then removed, cells were washed again with PBS and left to dry for 1 day before using them, to achieve the best result.

### 3. PDMS moulds with bioimprints

Once cells were fixed, PDMS prepolymer (Sylgard 184, Dow Corning) was mixed at a 10:1 w/w ratio, degassed, and poured on the fixed cells. This was followed by a further degassing step, curing at 37 °C overnight, and then peeling off. After separation, the PDMS mould with bioimprints was cleaned and further cross-linked by baking at 80 °C for 2 h. To fabricate casein with negative bioimprints, the initial PDMS mould was surface inactivated by treating it briefly with 0.1% w/w hydroxypropyl methylcellulose (HPMC, Sigma Aldrich, St. Louis, MO) solution in phosphate buffer for 10 min to ensure effective release of the secondary PDMS layer and then double-cast with additional PDMS prepolymer.

### 4. Transfer of bioimprints onto casein films

For casein films patterned with bioimprints, the same solution of noncrosslinked casein as for regular patterns (i.e., 15% casein in 0.2% NaOH mixed with 20% glycerol) was prepared. PDMS moulds were plasma-treated as described

above, and casein was liquid-cast onto the moulds. Casts were left to dry overnight at room temperature and then peeled off.

### D. Sample characterization

Photoresist, PDMS and casein samples were characterized using optical and differential interference contrast (DIC) microscopy (Olympus BX60 with Leica DFC320 imaging system), scanning electron microscopy (SEM, Raith150), and atomic force microscopy (AFM, Digital Instruments Dimension 3100). Recorded AFM images were analyzed using Gwyddion (V2.38). Casein samples were further characterized using UV–Vis spectrophotometry (Cary 6000i, Agilent) and contact angle measurement (CAM 2008, KSV Instruments).

## III. RESULTS AND DISCUSSION

### A. Casein optimization

Optimization of casein films plays an important role in the final result of the patterning process. Figure 2 shows the effect of the composition of the casein solution used for casting on final film formation. As can be seen in Fig. 2(a), casting of a solution of 10% casein in 0.2% NaOH, mixed with 10% glycerol produces clear, flexible films prior to cross-linking. For example, by increasing the casein concentration and omitting the plasticizer glycerol, the films become more brittle. In general, such non-cross-linked casein films took less than 2 h to dissolve in water and aqueous media. These observations match previously published data on plasticizer and cross-linking-dependent mechanical properties, as well

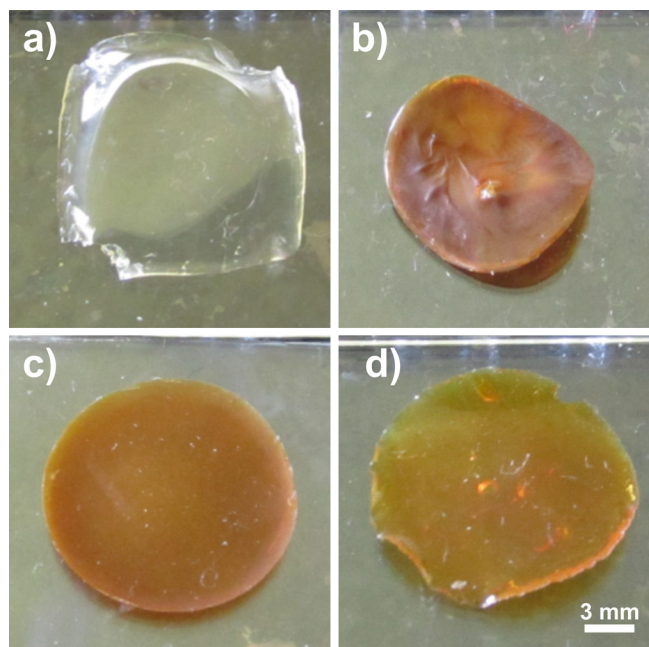


Fig. 2. (Color online) Casein films made with different methods: (a) Ten percent casein in 0.2% NaOH, mixed with 10% glycerol. (b) Fifteen percent casein in 3%  $\text{Na}_2\text{HPO}_4$ , no glycerol, immersed in 0.1% glutaraldehyde solution for 30 min. (c) Fifteen percent casein in 0.2% NaOH, mixed with 10% glycerol and 2% glutaraldehyde. (d) Fifteen percent casein in 0.2% NaOH, mixed with 20% glycerol, immersed in 3% citric acid solution for 30 min.

as the swelling behavior of such casein materials.<sup>17</sup> Thus, to use patterned substrates as tissue-culture substrates and as medical implants, devices need to be cross-linked to increase their stability. We found that films cross-linked by mixing 2% glutaraldehyde to the casting solution prior to casting showed superior long-term stability in excess of 2 weeks in aqueous media. Films made with this method initially expand 20% in diameter after immersion in media, which may influence secondary cells cultured on the films. Films cross-linked by citric acid<sup>18</sup> showed similar long term stability, but retained dimensional stability after immersion in media. Dissolution times in excess of 2 weeks are sufficient for *in vitro* tissue culture, and *in vivo* experiments in rats have indicated that GCC devices remain structurally intact up to 5–8 weeks after implantation.<sup>11</sup>

Figure 2(b) shows an example of a film produced using 15% casein in 3% Na<sub>2</sub>HPO<sub>4</sub>, and no glycerol, after immersing the dried film in 0.1% glutaraldehyde cross-linking solution for 30 min. The casein film appears brownish in color and shows bending due to cross-linking-induced mechanical stress. The brown color in this case is due to the glutaraldehyde cross-linker. The most suitable films regarding characteristics such as flexibility, low stress, and quality of pattern transfer were achieved by dissolving 15% casein in 0.2% NaOH solution, mixing with 15% glycerol, and cross-linking by mixing the solution with 2% glutaraldehyde. A circular substrate produced using this mixture is shown in Fig. 2(c).

At this concentration of glycerol, the film is still hydrophilic, as confirmed by a water contact angle of  $61.8 \pm 1.1^\circ$ . Films with 10% and 20% glycerol showed contact angles of  $55.2 \pm 2.2^\circ$  and  $101.9 \pm 0.3^\circ$ , respectively, the latter of which would be considered hydrophobic. In films cross-linked by citric acid, resolution is lost in the transfer process due to the need for baking the films at 150 °C for 1.5 h to complete the cross-linking process. Figure 2(d) shows an example of a casein film cast from 15% casein in 0.2% NaOH solution, mixed with 15% glycerol, and immersed in 3% citric acid solution for 30 min. The darker coloration in this case is due to the samples being baked at elevated temperature.

The effect of glutaraldehyde cross-linking on sample color was further investigated using UV–Vis spectrophotometry on samples with 15% casein content. Figure 3 shows transmission UV–Vis measurements of a non-cross-linked casein sample and samples of varying thickness (*t*) cross-linked with either 1% or 2% glutaraldehyde. As can be observed from the spectra, optical transmission in the visible range decreases significantly from non-cross-linked to cross-linked samples with a spectral shift corresponding to the sample color change from clear to orange-brown. It can also be seen that, while all cross-linked samples share the same characteristic spectral features, increasing the glutaraldehyde concentration from 1% to 2% for a similar thickness sample only has limited effect on transmission. Above 1.7 mm thickness, transmission is reduced to less than 15%, which will limit these devices to top-down microscopy for observing secondary cell growth.

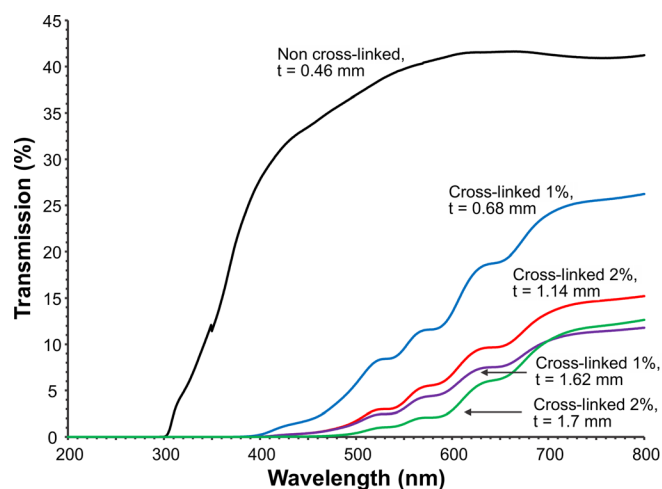


FIG. 3. (Color online) Transmission UV–Vis spectrophotometry measurements of various casein samples. Percentage glutaraldehyde concentration and sample thickness after drying (*t*) are indicated. Transmission in the visible range decreases significantly from non-cross-linked to cross-linked samples with a spectral shift corresponding to the sample color change from clear to orange-brown. Further increasing the glutaraldehyde concentration only has limited effect compared to sample thickness.

## B. Replication of regular features onto casein films

Regular micro- and nanofeatures were transferred from photoresist onto casein films by using the fabrication process described above. To investigate the quality of replication, a test pattern consisting of various geometric shapes, such as squares, circles, triangles, and arrays of these, was designed and transferred into casein. Pattern detail was analyzed using optical imaging and atomic force microscopy for the different replication steps. Figure 4 shows optical images of devices, and the test pattern captured at various stages of the process, beginning with the test pattern in photoresist on a silicon wafer. The test pattern contained various geometric shapes including a checkerboard array made up of  $15 \times 15 \mu\text{m}$  squares. As shown in Fig. 4(a), an array of nine copies of the test pattern was included on the initial wafer. The whole array was then transferred at wafer-level into PDMS, and the resulting intermediate stamp is shown in Fig. 4(b). This PDMS replication step has been associated with an average feature shrinkage ratio of 1.5% for curing at 80 °C,<sup>19</sup> which can be compensated for during the mask design. For replication into casein, the PDMS test pattern array was separated and then transferred into casein disks using 25 mm diameter stenciled PDMS wells.<sup>7</sup> Figure 4(c) shows a photograph of such a cured casein disk and the test pattern as a DIC micrograph (inset). Optical analysis of micron-scale patterns showed good agreement in lateral dimensions between master and replica when PDMS shrinkage was accounted for. However, we did observe some feature rounding in the vertical direction, as can be seen from the close-up of the square pixels of the checkerboard array in Fig. 4(d).

To investigate this further, and determine resolution limits of the process, we fabricated nanoscale test patterns using interference lithography. As shown in Fig. 5, both 500 nm wide parallel lines, as well as  $500 \times 500 \text{ nm}$  pixel arrays were produced in AZ1518 photoresist on silicon substrates.

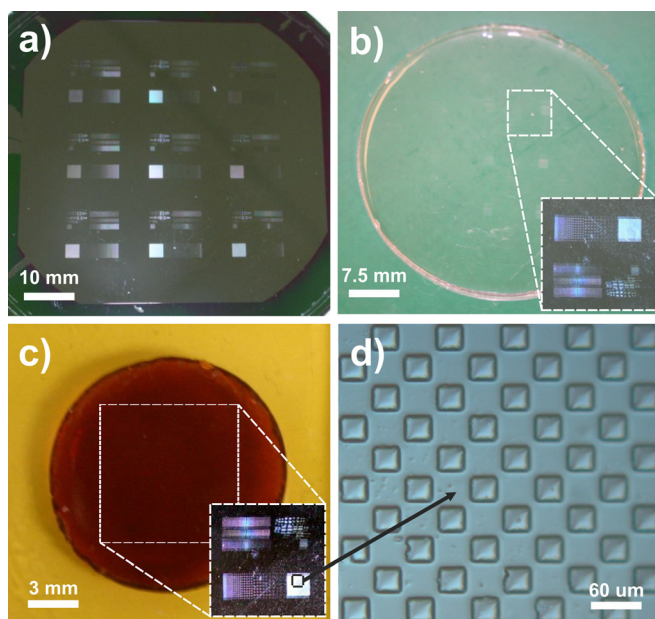


Fig. 4. (Color online) Replication of regular micron-scale geometries into casein: (a) Photograph of a  $3 \times 3$  array of AZ1518 photoresist patterns on 4 in. silicon wafer. (b) Photograph of a PDMS replica of the same wafer and close-up of one of the test patterns (inset). (c) Casein replica of one test pattern after removal from PDMS mould. Inset shows a DIC optical micrograph of the test pattern. (d) Optical micrograph of feature detail on the casein surface.

Replication of these line arrays into casein via PDMS intermediate moulds showed reasonable pattern fidelity with an average 10% dimensional shrinkage in depth of features, as shown in Fig. 5(a). Dot-arrays, which correspond to hole-arrays on the intermediate PDMS mould, did show a similar shrinkage in vertical direction and overall did not transfer well. Analysis of the shape of the casein replicas, shown on the right in Fig. 5(b), points toward the PDMS-casein casting step being resolution-limiting. The intermediate mould material PDMS itself has been shown capable of reproducing features down to 2 nm resolution<sup>20</sup> and we have previously demonstrated the transfer of features with nanometer resolution into PS using liquid-casting onto PDMS moulds.<sup>7</sup> One possible explanation for the distortions observed in the casein replicas may be related to limited wetting of the naturally hydrophobic PDMS mould by the aqueous casein solution during casting. Oxygen plasma treatment is used prior to casein application; however, this surface modification has a limited temporal stability. Thus, we are currently investigating the use of more permanent treatments to reduce the surface energy of the mould, such as the use of polyvinylpyrrolidone,<sup>21</sup> which may help to improve resolution.

### C. Replication of bioimprints onto casein films

The exact replication of cellular morphology into a biodegradable and renewable material such as casein could significantly improve its application as substrate in tissue engineering and as structural material in implants. By integrating bioimprinted features, surfaces of engineered devices can be made to influence the phenotype of adjacent cells and thus influence

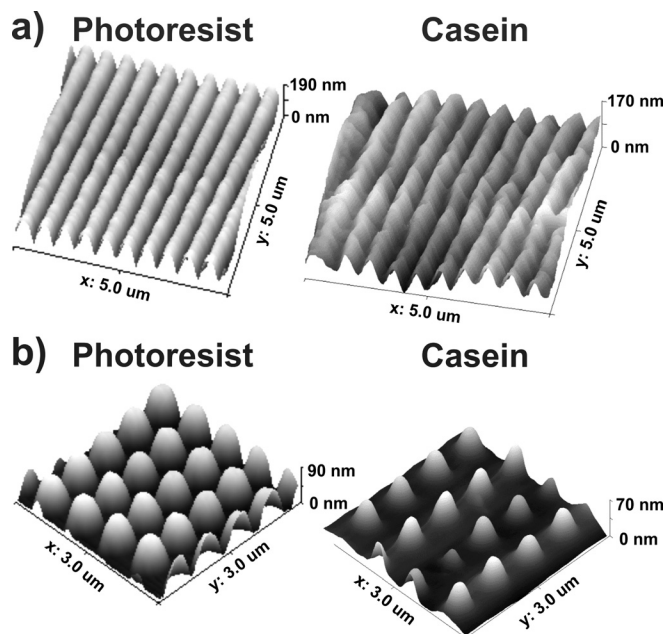


Fig. 5. Replication of regular nanoscale geometries into casein: (a) AFM images of 500 nm wide line arrays fabricated in AZ1518 photoresist using interference lithography (left) and the respective casein replica (right). (b) AFM images of  $500 \times 500$  nm dot arrays fabricated in AZ1518 photoresist using  $90^\circ$  rotated double-exposure interference lithography (left) and the respective casein replica (right).

cell and tissue growth outcomes.<sup>8,22–24</sup> Since casein degrades in media and tissue, the need for further surgery to take out the implant can be eliminated. By optimizing the cross-linking physical properties, the degradation times can be controlled.<sup>17</sup> In the case of tissue engineering, degradable substrates would enable the gradual release of engineered tissue from the culture platform after substrate topography has been used to influence cell alignment and phenotype.<sup>6</sup>

To demonstrate the fabrication of casein devices with cell-like geometries, we cultured muscle cells (C2C12 myoblasts) for 24 h on glass microscope slides with  $2.5 \mu\text{m}$  deep, etched alignment grids. The C2C12 myoblast cell line was chosen, as it is a useful tool to study differentiation (myoblast and osteoblast), protein expression, and mechanistic pathways.<sup>25</sup> We have previously shown that bioimprinting of this cell line can be used to produce PS substrates with topographies corresponding to cell morphologies at different differentiation time-points.<sup>5</sup> Alignment grids were integrated into the glass microscope slides to facilitate the direct comparison of the same cells during initial culture, once bioimprinting into the PDMS intermediate mould and after the final transfer into casein. These grids would be omitted for tissue-culture substrates as they constitute surface patterns themselves, which may influence cell growth.

Figure 6 shows an example of the same cluster of C2C12 cells imaged using DIC optical microscopy at each of these stages. The general orientation of the cluster after bioimprinting into PDMS, as shown in Fig. 6(b), is mirrored compared to the actual cell-culture shown in Fig. 6(a). This is due to the cell imprints in PDMS being a negative image of the original. In related work on PS, we have observed

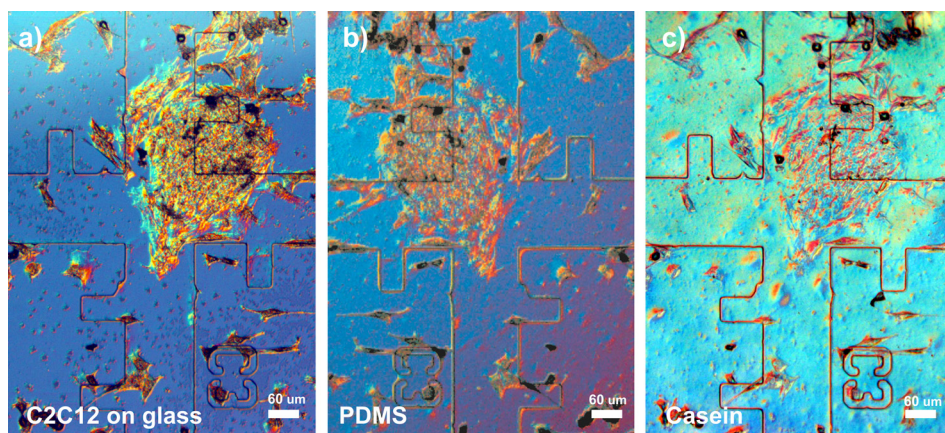


FIG. 6. (Color online) Replication of cellular features into casein film using bioimprint: DIC optical micrographs of fixed C2C12 mouse myoblast cells (a) on the glass microscope slide prior to imprinting, (b) replicated into PDMS (negative), and (c) casein (positive) film. The alignment grid used for cell registration between imprint steps is etched into the glass microscope slide and transfers as part of the cell replication process.

distinct differences in morphology and growth rates depending on whether human nasal chondrocytes<sup>7</sup> or endometrial cancer cells<sup>26</sup> were grown on negative or positive bioimprints. Both polarities can be transferred into casein using PDMS double-casting, which has been found to generate average replication errors of less than 4%.<sup>27</sup> Once the PDMS mould is obtained, repeated cleaning of the replica with 10% SDS/HCl and 1% trypsin-EDTA was used to ensure that no biological material remains on the mould and only topographical information is transferred. Figure 6(c) shows the final positive casein replica of the same area as in Figs. 6(a) and 6(b). General cell outlines and morphological details, such as bilateral myoblast extension using long thin lamellipodia extended in one or opposite directions to network with adjacent cells, are transferred and can be observed on the casein surface.

AFM images of the negative replica in PDMS and positive replica in casein of the same cell are shown in Fig. 6. Insets in Figs. 7(a) and 7(b) show optical micrographs illustrating that these scans are performed in exactly the same location of the cell-culture on both materials. As can be observed in Fig. 7(a), the scans show that the negative PDMS replica contains cellular details down to the nanometer range. Larger micron-scale physiological cell-structures are clearly visible, such as connecting lamellipodia and the outline of the cell nucleus, as well as nanometer-sized detail on the cell-membrane, which has previously been attributed to exocytosis events and fusion pores.<sup>4,28</sup> However, the AFM scan of the same area after replication into casein, shown in Fig. 7(b), exhibits significantly less nanometer-scale detail. While the overall topography and micron-sized detail, including larger lamellipodia, are transferred with an average reduction in depth similar to regular features ( $\sim 7\%$ ), cell structures at the smallest end of dimensional accuracy are lacking in definition. As explained prior in the regular patterning section, this reduction in resolution from PDMS to casein may be related to the hydrophobicity of the surface of PDMS and thus high wetting angle for the casein solution.

In general, casein substrates produced using this process contain biologically relevant cell features in defined regions

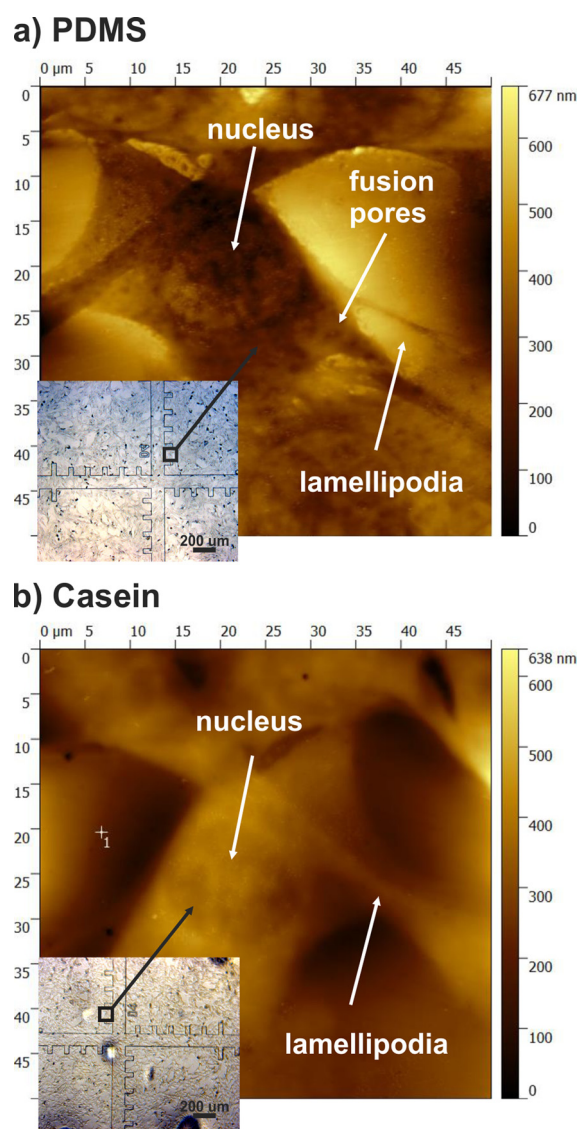


FIG. 7. (Color online) Atomic force microscopy images of the replication of a single cell into casein: (a) negative cell replica bioimprinted into the PDMS master and (b) positive cellular imprint into the final casein film. Insets show optical micrographs of the corresponding scan position on the PDMS and casein replicas identified using the alignment grid.

on a substrate with known, homogeneous surface chemistry and the added benefit of biodegradability. To improve the resolution we are currently investigating a mixture of alternative PDMS surface treatments, as well as the addition of a degassing step to the casein casting process. We have also begun to evaluate the use of these bioimprinted substrates for cell–substrate applications in comparison with lithographically patterned and flat, nonpatterned casein cell-culture substrates. Initial results indicate that the choice of cross-linker and cross-linking method may be crucial, since glutaraldehyde, as used for implanted casein devices, may not be suitable for cell-culture substrates due to it leaching into the cell-culture media. Commonly employed as a cell fixant, glutaraldehyde negatively influences secondary C2C12 cell growth and an alternative enzyme-catalyzed crosslinking approach may be more suitable.<sup>29</sup>

#### IV. SUMMARY AND CONCLUSION

We have shown the successful replication of micro- and nanostructured regular and bioimprinted surface features onto the surface of free-standing casein devices. To the best of our knowledge, this is the first time liquid-casting of casein solution onto PDMS intermediate moulds was used to demonstrate feature transfer down to the micron-scale. Replication of regular nanoscale features showed some lateral feature distortion, which was attributed to reduced wetting of the smallest features on the hydrophobic PDMS moulds. Mouse myoblast cells were successfully bioimprinted using PDMS and the cell morphology transferred into casein. Comparison of optical micrographs and AFM images of cells at various stages during the replication process demonstrated the transfer of features with high resolution. We are currently investigating the culture of secondary cells on the patterned casein substrates and their controlled degradation in culture media, which would enable widespread uptake of this biomimetic technology for the fabrication of degradable orthopedic implants and tissue engineering substrates.

#### ACKNOWLEDGMENTS

The authors would like to thank Helen Devereux and Gary Turner for technical assistance, Alana Hyland for help with the spectrophotometry, Ken Morrison and Xiao Wei Tew for help with the contact angle measurements, and Kenny Chitcholtan and John Evans for help with cell-culture. Financial support for this work was provided by the MacDiarmid Institute for Advanced Materials and Nanotechnology and the University of Canterbury through the Biomolecular Interaction Centre.

- <sup>1</sup>R. J. McMurray *et al.*, *Nat. Mater.* **10**, 637 (2011).
- <sup>2</sup>H. Jeon, C. G. Simon, and G. Kim, *J. Biomed. Mater. Res. B Appl. Biomater.* **102**, 1580 (2014).
- <sup>3</sup>V. Nock, L. M. Murray, C. Dennis, J. J. Evans, and M. M. Alkaiasi, “Effect of micro-patterned polystyrene substrates on myoblast morphology,” *paper presented at the 6th International Conference on Advanced Materials and Nanotechnology*, Auckland, New Zealand (2013).
- <sup>4</sup>J. J. Muys, M. M. Alkaiasi, D. O. S. Melville, J. Nagase, P. Sykes, G. Parguez, and J. J. Evans, *J. Nanobiotechnol.* **4**, 1 (2006).
- <sup>5</sup>L. M. Murray, V. Nock, M. M. Alkaiasi, J. J. M. Lee, and T. B. F. Woodfield, *J. Vac. Sci. Technol., B* **30**, 06F902 (2012).
- <sup>6</sup>L. Murray, V. Nock, J. Evans, and M. Alkaiasi, *J. Nanobiotechnol.* **12**, 60 (2014).
- <sup>7</sup>I. Mutreja, T. B. F. Woodfield, S. Sperling, V. Nock, J. J. Evans, and M. M. Alkaiasi, *Biofabrication* **7**, 025002 (2015).
- <sup>8</sup>W. Y. Tong *et al.*, *Biomaterials* **33**, 7686 (2012).
- <sup>9</sup>A. Ballo, H. Agheli, J. Lausmaa, P. Thomsen, and S. Petronis, *Int. J. Nanomed.* **6**, 3415 (2011).
- <sup>10</sup>M. N. Belgacem and A. Gandini, *Monomers, Polymers and Composites from Renewable Resources* (Elsevier Science, Oxford, UK, 2011).
- <sup>11</sup>W. Wang, J.-H. Lin, C.-C. Tsai, H.-C. Chuang, C.-Y. Ho, C.-H. Yao, and Y.-S. Chen, *Macromol. Biosci.* **11**, 914 (2011).
- <sup>12</sup>B. Dhandayuthapani, Y. Yoshida, T. Maekawa, and D. S. Kumar, *Int. J. Polym. Sci.* **2011**, 290602.
- <sup>13</sup>P. Müller-Buschbaum, R. Gebhardt, E. Maurer, E. Bauer, R. Gehrke, and W. Doster, *Biomacromolecules* **7**, 1773 (2006).
- <sup>14</sup>H. Juvonen, M. Smolander, H. Boer, J. Pere, J. Buchert, and J. Peltonen, *J. Appl. Polym. Sci.* **119**, 2205 (2011).
- <sup>15</sup>A. Hashemi, D. Tay, I. Mutreja, M. A. Ali, M. M. Alkaiasi, and V. Nock, “Micro- and Nano-Patterning of Freestanding Protein Films,” *paper presented at the 7th International Conference on Advanced Materials and Nanotechnology*, Nelson, New Zealand (2015).
- <sup>16</sup>S. Sivasubramaniam and M. M. Alkaiasi, *Microelectron. Eng.* **119**, 146 (2014).
- <sup>17</sup>A. Ghosh, M. A. Ali, and G. J. Dias, *Macromolecules* **10**, 1681 (2009).
- <sup>18</sup>Y. Yang and N. Reddy, *Int. J. Biol. Macromol.* **51**, 37 (2012).
- <sup>19</sup>S. Lee and S. Lee, *Microsyst. Technol.* **14**, 205 (2008).
- <sup>20</sup>F. Hua *et al.*, *Nano Lett.* **4**, 2467 (2004).
- <sup>21</sup>S. Hemmilä, J. V. Cauich-Rodríguez, J. Kreutzer, and P. Kallio, *Appl. Surf. Sci.* **258**, 9864 (2012).
- <sup>22</sup>M. Karlsson, F. Johansson, and M. Kanje, *Acta Biomater.* **7**, 2910 (2011).
- <sup>23</sup>S. Chen, J. A. Jones, Y. Xu, H.-Y. Low, J. M. Anderson, and K. W. Leong, *Biomaterials* **31**, 3479 (2010).
- <sup>24</sup>W. B. David and T. Liping, “Effect of microtopography on fibrocyte responses and fibrotic tissue reactions at the interface,” in *Proteins at Interfaces III State of the Art* (American Chemical Society, Washington, DC, USA, 2012), Vol. 1120, p. 339.
- <sup>25</sup>S. N. Stephansson, B. A. Byers, and A. J. García, *Biomaterials* **23**, 2527 (2002).
- <sup>26</sup>T. Tan, P. Sykes, M. M. Alkaiasi, and J. J. Evans, “Cancer cell behaviours on a culture substrate imprinted with their own features,” *paper presented at the 5th Annual Symposium on Physics of Cancer*, Leipzig, Germany (2014).
- <sup>27</sup>L. Yang, X. Hao, C. Wang, B. Zhang, and W. Wang, *Microsyst. Technol.* **20**, 1933 (2014).
- <sup>28</sup>F. Samsuri, J. S. Mitchell, M. M. Alkaiasi, and J. J. Evans, *J. Nanotechnol.* **2009**, 6.
- <sup>29</sup>T. Heck, G. Faccio, M. Richter, and L. Thöny-Meyer, *Appl. Microbiol. Biotechnol.* **97**, 461 (2013).